4-Azahomoadamant-3-ene: Spectroscopic Characterization and Photoresolution of a Highly Reactive Strained Bridgehead Imine

Juliusz G. Radziszewski,[1a] John W. Downing,[1a] Mikolaj Jawdosiuk,[1b] Peter Kovacic,[1b] and Josef Michl*[1a]

Contribution from the Departments of Chemistry, University of Utah, Salt Lake City, Utah 84112, and University of Wisconsin, Milwaukee, Wisconsin 53201.
Received June 27, 1984

Abstract: Low-temperature irradiation of 1-azidoadamantane in argon, nitrogen, 3-methylpentane, or polyethylene matrices or as neat solid produced (i) the diamagnetic highly reactive strained bridgehead imine, 4-azahomoadamant-3-ene, characterized by its vibrational (Raman, IR) and electronic (UV absorption, CD) spectra, (ii) traces of 1-adamantylnitrene, detected by EPR spectroscopy and by photochemical trapping with CO, and (iii) molecular nitrogen, detected by Raman spectroscopy. A warm-up in any of the matrices produced the known dimer of the imine. In an argon matrix or in the neat solid, dimerization was observed to proceed rapidly already at about 60 K. Optical resolution of the bridgehead imine to 2% optical purity was achieved by irradiation with circularly polarized 308-nm laser light, preferably in polyethylene between 160 and 200 K where rotational diffusion of the imine is fast and translational diffusion still slow. The activation energy for thermal racemization is believed to be at least 17 kcal/mol since no racemization was detected up to 220 K, at which temperature dimerization in the polyethylene matrix begins to be significant. Interpretation of the results is based on calculations by MNDO and INDO/S methods and suggests that the torsion angle of the severely distorted C=N moiety is 50 ± 10°.

In recent years, "anti-Bredt"[2] strained bridgehead imines have been attracting increasing attention.[3-15] Several representatives of this class of compounds have apparently been generated upon irradiation of suitable azides in fluid solutions, since the expected dimeric or trapping products were formed.[4-13] However, only the relatively strain-free 2-azabicyclo[3.3.1]nonene has been isolated as a stable compound.[3]

In a preliminary report,[14] we have described the first direct observation of a highly strained and reactive bridgehead imine, 4-azahomoadamant-3-ene (**1**), using matrix-isolation IR, Raman, UV and CD spectroscopy. We have since extended this work to several additional strained bridgehead imines.[15] Two other research groups have recently reported matrix-isolation IR spectra of two of these imines, one obtained from 1-azidonorbornane[16] and one from 1-azido-4-methylbicyclo[2.2.2]octane.[17]

Interest in the spectral properties and reactivity of strained C=N double bonds is partly motivated by the ability of this chromophore and its more complicated conjugated derivatives to participate in thermal and photochemical syn-anti and cis-trans isomerization processes such as those believed to be involved in vision.[18] The paths followed in many of the photochemical isomerization processes most likely pass through nonplanar geometries similar to those expected in the bridgehead imines. Several reviews on the spectroscopic and photochemical properties of the C=N chromophore are available,[19-23] as are quantum chemical calculations at various levels of sophistication.[14,24-28] An intriguing picture is beginning to emerge from these calculations, since the availability of the "lone-pair" orbital on the nitrogen atom makes the electronic states involved more complicated than those involved in the cis-trans isomerization of olefins.

The overall goal of our investigations is to reach an understanding of the molecular and electronic structure and the reactivity of the C=N bond as a function of the torsion angle, the C=N—C valence angle, and the degree of pyramidalization on the carbon and to make comparisons with similarly distorted C=C bonds. This is to be accomplished by investigating a series of molecules with increasingly distorted bridgehead C=N bonds. The isolated C=N moiety is simple enough for high-quality quantum mechanical calculations on a model such as CH_2=NH, but calculations useful for the spectroscopy of the actual bridgehead imines are presently limited to the semiempirical or empirical varieties.

We are further interested in the mechanism of the photochemical azide to imine transformation[29] and in the possible involvement of nitrenes as intermediates or side products.

In the present paper, we provide a full account of the preparation and the observed spectra of matrix-isolated 4-azahomo-

(1) (a) University of Utah. (b) University of Wisconsin.
(2) Bredt, J.; Thouet, H.; Schmitz, J. *Justus Liebigs Ann. Chem.* **1924**, *437*, 1.
(3) Toda, M.; Hirata, Y.; Yamamura, S. *Chem. Commun.* **1970**, 1597; *Tetrahedron* **1972**, *288*, 1477.
(4) Reed, J. O.; Lwowski, W. *J. Org. Chem.* **1971**, *36* 2864.
(5) Quast, H.; Eckert, Ph. *Liebigs Ann. Chem.* **1974**, 1727.
(6) Quast, H.; Eckert, Ph. *Angew. Chem., Int. Ed. Engl.* **1976**, *15*, 168.
(7) Sasaki, T.; Eguchi, S.; Hattori, S.; Okano, T. *J. Chem. Soc., Chem. Commun.* **1981**, 1193.
(8) Becker, K. B.; Gabutti, C. A. *Tetrahedron Lett.* **1982**, 1883.
(9) Quast, H.; Seiferling, B. *Liebigs Ann. Chem.* **1982**, 1553.
(10) Sasaki, T.; Eguchi, S.; Okano, T. *J. Org. Chem.* **1981**, *46*, 4474.
(11) Sasaki, T.; Eguchi, S.; Okano, T. *Tetrahedron Lett.* **1982**, *23*, 4969.
(12) Sasaki, T.; Eguchi, S.; Okano, T. *J. Am. Chem. Soc.* **1983**, *105*, 5912.
(13) Sasaki, T.; Eguchi, S.; Okano, T.; Wakata, Y. *J. Org. Chem.* **1983**, *48*, 4067. Jawdosiuk, M.; Kovacic, P. *J. Chem. Soc., Perkin Trans. 1* **1984**, 2583. Sasaki, T.; Eguchi, S.; Okano, T. *J. Org. Chem.* **1984**, *49*, 444.
(14) Michl, J.; Radziszewski, G. J.; Downing, J. W.; Wiberg, K. B.; Walker, F. H.; Miller, R. D.; Kovacic, P.; Jawdosiuk, M.; Bonacic-Koutecky, V. *Pure. Appl. Chem.* **1983**, *55*, 315.
(15) Obtained from 1-azidonoradamantane, 1-azidonorbornane, 1-azidobicyclo[2.2.2]octane, 1-azidobicyclo[2.1.1]hexane, and 1-azido-3-methylbicyclo[1.1.1]pentane: Radziszewski, J. G.; Downing, J. W.; Wentrup, C.; Kaszynski, P.; Jawdosiuk, M.; Kovacic, P.; Michl, J. *J. Am. Chem. Soc.* **1984**, *106*, 7996 and unpublished results.
(16) Sheridan, R. S.; Ganzer, G. A. *J. Am. Chem. Soc.* **1983**, *105*, 6158.
(17) Dunkin, I. R.; Shields, C. J.; Quast, H.; Seiferling, B. *Tetrahedron Lett.* **1983**, 3887.
(18) Harbison, G. S.; Smith, S. O.; Pardoen, J. A.; Winkel, C.; Lugtenburg, J.; Herzfeld, J.; Mathies, R.; Griffin, R. G. *Proc. Natl. Acad. Sci. U.S.A.* **1984**, *81*, 1706. Smith, S. O.; Myers, A. B.; Pardoen, J. A.; Winkel, C.; Mulder, P. P. J.; Lugtenburg, J.; Mathies, R. *Proc. Natl. Acad. Sci. U.S.A.* **1984**, *81*, 2055.
(19) Paetzold, R.; Reichenbacher, M.; Appenroth, K. *Z. Chem.* **1981**, *21*, 421.
(20) Padwa, A. *Chem. Rev.* **1977**, *77*, 37.
(21) Pratt, A. C. *Chem. Soc. Rev.* **1977**, *6*, 63.
(22) Patai, S.; Ed. "The Chemistry of the Carbon-Nitrogen Double Bond"; Interscience Publishers: New York, 1970.
(23) Sandorfy, C. *Top. Curr. Chem.* **1979**, *86*, 91. In particular, see p 132.
(24) Howell, J. M. *J. Am. Chem. Soc.* **1976**, *98*, 886.
(25) Macaulay, R.; Burnelle, L. A.; Sandorfy, C. *Theor. Chim. Acta* **1973**, *29*, 1.
(26) Osamura, Y.; Kitaura, K.; Nishimoto, K.; Yamabe, S. *Chem. Phys. Lett.* **1979**, *63*, 406.
(27) Russegger, P. *Chem. Phys.* **1978**, *34*, 329.
(28) Bonacic-Koutecky, V.; Persico, M. *J. Am. Chem. Soc.* **1983**, *105*, 3388.
(29) Moriarty, R. M.; Reardon, R. C. *Tetrahedron* **1970**, *26*, 1379. Kyba, E. P.; Abramovitch, R. A. *J. Am. Chem. Soc.* **1980**, *102*, 735.

0002-7863/85/1507-0594$01.50/0

Chart I

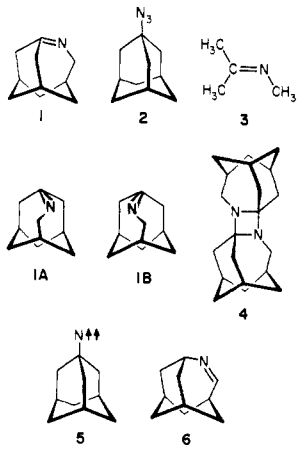

adamant-3-ene (**1**). Our initial choice of this particular bridgehead imine for the first detailed investigation was based on the results of earlier room-temperature investigations:[5] there was reason to believe that 1-azidoadamantane (**2**) photochemically rearranges to **1** at room temperature, the threefold symmetry of the adamantyl substituent promised the clean formation of a single product since it does not matter which C–C bond shifts, and **1** was clearly strained enough to be interesting since it was not isolable in substance at room temperature, similar to its hydrocarbon analogue,[30] homoadamant-3-ene. There also was reason to expect the azide photorearrangement to proceed in low-temperature matrices since the irradiation of *tert*-butyl azide in a nitrogen matrix had been shown[31] to produce the expected *N*-methylisopropylidene imine (**3**).

Results and Discussion

Preparation and Identification of 4-Azahomoadamant-3-ene (1). In an argon or nitrogen matrix at 12–17 K (matrix ratio higher than 250:1), in a 3-methylpentane (3-MP) glass at 77 K, and in a solid solution inside a polyethylene (PE) sheet at 12 K, the UV spectrum of **2** is characterized by a relatively weak absorption band with a maximum at 286 nm (in PE, $\epsilon \doteq 28$). Solid argon, nitrogen, and 3-MP are used commonly for low-temperature isolation of reactive species, while polyethylene has been used much less. This medium, while more reactive than argon or nitrogen, also offers several advantages. It is easy to work with, yields reproducible absorption base lines, and can be used over a wide temperature range. It is isotropic and, in combination with perdeuterated polyethylene, it is transparent from far-IR to the edge of vacuum UV. Of course, the use of stretched polymers as orienting matrices is widespread.[32]

In any of these four environments, upon irradiation with a low-pressure mercury arc (254 nm) or, much faster, with the 308-nm line of a XeCl excimer laser, the 286-nm absorption band of **2** gradually disappeared and two new absorption peaks appeared: a weaker one at 302 nm (Ar, N_2) or 300 nm (3-MP, PE, $\epsilon \doteq 245$) and a stronger one at 214 nm (PE, $\epsilon \doteq 2850$). The UV spectrum is shown in Figure 1. Virtually complete conversion to the photoproduct was achieved after several hours of irradiation. This is difficult to ascertain from the strongly overlapping UV spectra but is obvious from the vibrational spectra described below. The spectrum of the photoproduct appeared to be stable indefinitely at the low temperatures used. The product was also very stable to further irradiation at 254 nm and apparently indefinitely stable to irradiation with the 308-nm line of XeCl excimer laser. Extremely slowly at 254 nm, and somewhat faster at shorter wavelengths, it undergoes further phototransformations (see below).

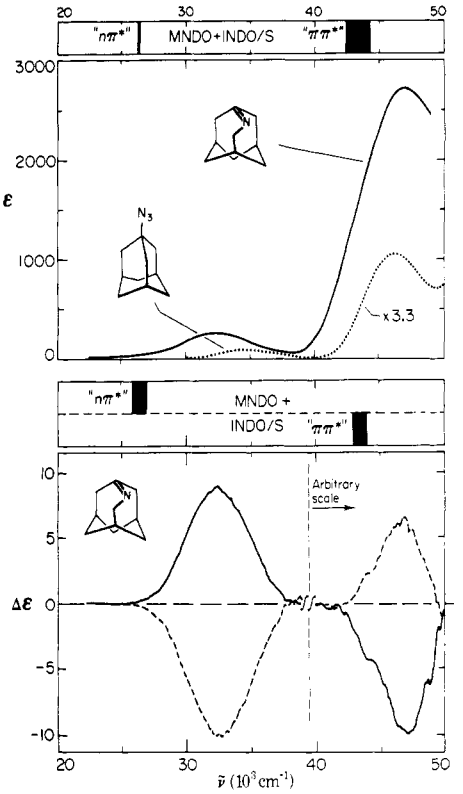

Figure 1. Base-line corrected UV absorption spectra of **1** and **2** at 12 K (top) and CD spectrum of **1** at 200 K (bottom). Polyethylene matrix. The $\Delta\epsilon$ scale corresponds to pure enantiomers, but the actual measurement was performed on a sample of 2% optical purity after photoresolution with right-handed (full line) or left-handed (dashed line) circularly polarized light (see text). Results of an INDO/S calculation at MNDO-optimized geometry of **1** are also shown. Line thickness indicates relative magnitudes of oscillator and rotatory strengths of the two transitions (see Table II).

Efforts to detect a fluorescence or phosphorescence emission spectrum of the photoproduct in argon or nitrogen matrix upon excitation at 300 nm failed. If any emission is present, it is extremely weak or lies beyond the detection limit of the S-20 response photomultiplier used.

Simultaneously with UV absorption measurements, we have performed IR absorption measurements using the same samples in argon, nitrogen, and polyethylene matrices and also in neat polycrystalline **2**. Before irradiation, the spectra of **2** showed the characteristic[33a] vibrations of the azido group at 2094 cm^{-1} (antisymmetric stretch), 1247 cm^{-1} (symmetric stretch), and 737 cm^{-1} (bend). During the irradiation, the bands of **2** gradually decreased in intensity until they eventually disappeared. In their place, a single new set of absorption peaks grew, among which a doublet at 1600 and 1608 cm^{-1} (in argon) was by far the strongest, except for the C–H stretch bands near 3000 cm^{-1}. No absorption bands grew in above 3000 cm^{-1}. This new set of IR bands grew in at the same rate as the UV peak at 302 nm, and we concluded that it belongs to the same species.

The same samples isolated in an argon matrix, a nitrogen matrix, and a polyethylene matrix at 12 K which were used in the UV and IR experiments were also used to record the Raman spectra. The spectrum of **2** shows the expected bands, coincident in frequency with those observed in the IR spectrum but with different relative intensities. Upon irradiation the Raman bands of the azide **2** disappeared simultaneously with its UV and IR bands and were gradually replaced by a set of bands at locations identical with those observed in the IR spectrum of the photoproduct, but again with a different intensity distribution. In the argon and polyethylene matrices, a sharp band gradually appeared at 2323 cm^{-1} at the same time. This band is assigned to the Raman peak of molecular nitrogen. Control experiments showed that it is not due to atmospheric nitrogen leaking into the appa-

(30) Martella, D. J.; Jones, M., Jr.; Schleyer, P. v. R.; Maier, W. F. *J. Am. Chem. Soc.* **1979**, *101*, 7634.
(31) Dunkin, I. R.; Thomson, P. C. P. *Tetrahedron Lett.* **1980**, *21*, 3813.
(32) For a recent example, see: Thulstrup, E. W.; Michl, J. *J. Am. Chem. Soc.* **1982**, *104*, 5594.

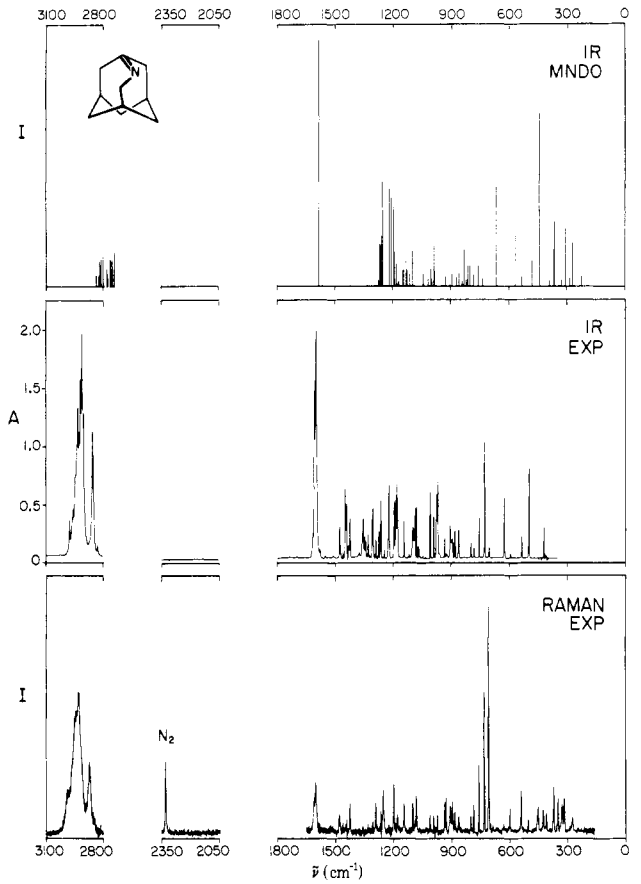

Figure 2. Raman scattering intensity (bottom) and infrared absorbance (center) of **1** in an argon matrix at 12 K. The IR spectrum calculated by the MNDO method is shown on top (frequencies scaled by 0.854, see text). Only relative intensities are shown.

ratus. Figure 2 presents a comparison of the IR and Raman spectra of the photoproduct in argon matrix.

The IR and Raman measurements were repeated with **2** labeled with a single ^{15}N atom in the azido group, distributed equally between the terminal position and the position attached to carbon. In comparison with the spectra of the unlabeled azide **2**, those of the two isotopomeric labeled azides showed shifts for the characteristic vibrations of the azido group but the frequencies of other vibrations were virtually unchanged. Now, the antisymmetric stretch at 2094 cm^{-1} was shifted to 2084 and 2071 cm^{-1} and the symmetric stretch at 1247 cm^{-1} to 1238 and 1222 cm^{-1}. The bend at 737 cm^{-1} now occurred at 737 and 732 cm^{-1}. The behavior upon photolysis was unchanged by the labeling, except that upon close inspection, many bands of the photoproduct now appeared as doublets of equal intensity. By far, the largest splitting was observed (i) for the intense bands of the photoproduct located at 1600 and 1608 cm^{-1} in the natural abundance spectra, where ^{15}N bands now appeared at 1575 and 1582 cm^{-1} both in IR and in Raman spectra, and (ii) for the peak assigned to molecular nitrogen in the Raman spectrum, where peaks were now present at 2288 and 2323 cm^{-1} as expected for a 1:1 mixture of $^{14}N_2$ and $^{14}N^{15}N$. Selected examples of the isotopic doublets are shown in Figure 3.

Except for very small solvent shifts, the UV, IR, and Raman spectral observations were the same in all of the matrices used. They are compatible with the assignment of the structure of the observed organic photoproduct as the bridgehead imine **1**, 4-azahomoadamant-3-ene, formed from the azide **2** by a loss of molecular nitrogen and bond migration. The N_2 product has been detected unequivocally, and the properties of the organic product are those expected:

(i) The weak UV band near 300 nm ($\epsilon_{max} \doteq 245$) is analogous to the $n\pi^*$ transition of ordinary planar trisubstituted imines ($\lambda_{max} \doteq 240$ nm, $\epsilon_{max} \doteq 200$).[20] The far more intense absorption near

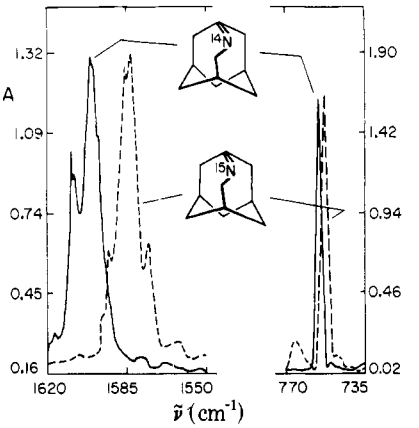

Figure 3. Segments of the IR spectra of **1** (full line) and **1**-^{15}N (dashed line) in argon matrix at 12 K. Vertical scale: absorbance.

214 nm ($\epsilon_{max} \doteq 2850$) is analogous to the less well documented $\pi\pi^*$ transition of planar imines ($\lambda_{max} \doteq 180$ nm, $\epsilon_{max} \doteq 10^4$).[20] The red shifts of both bands relative to their position in planar imines are as anticipated. Their very broad and structureless shapes are compatible with the expected short lifetime and very large difference between the equilibrium geometries of the ground and excited electronic states (see below).

(ii) The vibration near 1600 cm^{-1}, relatively intense in the IR and relatively weak in the Raman spectrum, and shifted by 18 cm^{-1} to lower frequencies in the ^{15}N-labeled material, is analogous to the C=N stretch of such imines (1669 cm^{-1} in **3**[31]). The difference between **1** and **3** is in the expected direction, and the isotopic shift has the anticipated[34] magnitude.

In agreement with prior observations on *tert*-butyl azide[31] and with less direct evidence obtained for other azides,[29] we have observed no indications of the involvement of a discrete intermediate, such as a nitrene, under the conditions used in these UV, IR, and Raman experiments. However, our results do not exclude the possibility that such an intermediate intervenes at some point along the path of the photochemical transformations of **2** into **1**.

Spectroscopic measurements alone can rarely be relied upon to provide unequivocal structural evidence for matrix-isolated molecules of the size of **1**, and complementary chemical trapping evidence is usually considered essential. In our case, this is provided by the self-trapping of **1** to produce the known[5] dimer **4**. When a polyethylene sheet containing **1** was warmed up to about 280 K, the UV as well as IR absorption bands of **1** were observed to disappear gradually. Simultaneously, a new set of IR bands grew in (Figure 4). These were identical with those of the authentic dimer, the diazetidine **4**. Afterward, no UV absorption was detectable above 200 nm. Similar changes in the UV spectra were observed when a 3-methylpentane glass containing **1** was melted. When a nitrogen or argon matrix was gradually warmed up after photolysis, the quality of the recorded UV and IR spectra deteriorated until all gas was gone and only a white powder remained on the substrate plate. After complete warm-up, the same white crystalline solid was isolated from each of these four media. Its IR spectrum and its mass spectrum were both identical with those of an authentic sample of the 4-azahomoadamant-3-ene dimer **4**.[5] This dimer appears to be the only product of a slow warm-up if the photoconversion was complete, with two exceptions. First, in the 3-MP glass experiment, a very small amount of yellow impurity was also produced. Second, when **1** was produced by irradiation of a neat solid film of **2** (~95% conversion) and subsequently warmed up, dimer formation became noticeable in the IR spectra at temperatures as low as 60 K. This is also the temperature at which noticeable dimerization is observed

(33) Bellamy, L. J. "The Infrared Spectra of Complex Molecules"; 3rd ed.; Wiley: New York, **1975**; Vol. 1, (a) p 305, (b) p 298. Horak, M.; Papousek, D. "Infracervena Spectra a Struktura Molekul"; Academia: Prague, **1976**; (a) p 737, (b) p 741.

(34) Pinchas, S.; Laulicht, I. "Infrared Spectra of Labeled Compounds"; Academic Press: London, **1971**; p 216.

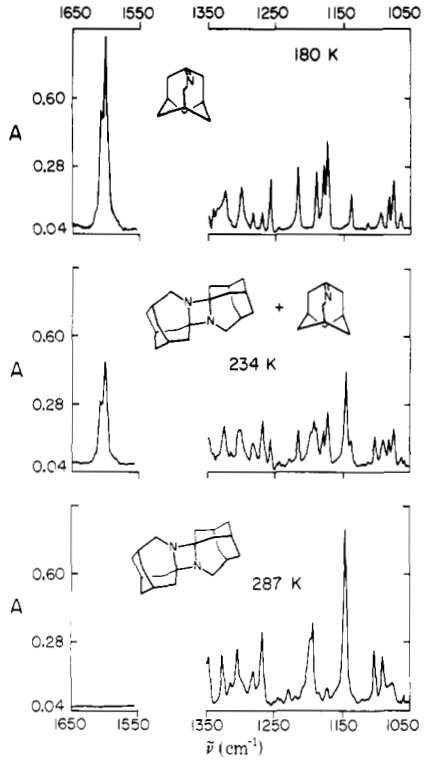

Figure 4. Segments of the IR spectrum of **1** (absorbance) taken in a polyethylene matrix (polymer absorption subtracted) at three temperatures during warm-up.

by IR when **1** is isolated in an argon matrix. In neat solid film, the dimer **4** was not the only product observed by IR spectroscopy. The nature of the additional product or products is still under investigation.

The ease with which **1** dimerizes is striking. However, the reaction is most likely not a formally orbital-symmetry-forbidden 2s + 2s process, and orbital interaction schemes in which the nitrogen lone-pair orbitals participate can readily be envisaged.

Adamantylnitrene (5)—A Minor Byproduct. Although we were not able to detect any evidence for more than a single primary organic photoproduct in the UV, IR, and Raman spectra, such evidence was obtained from ESR measurements. A weak ESR signal at 8210 G (at a klystron frequency of 9.3 GHz) appeared when the azide **2** was irradiated in argon at 12 K (Figure 5). Unlike the UV, IR, and Raman signals of **1**, the ESR signal grew faster when the low-pressure mercury lamp (254 nm) rather than when the 308-nm laser line was used for the irradiation. It reached a maximum in a few hours of 254 nm irradiation and then slowly decayed as irradiation continued. In this manner, it was possible to destroy the ESR signal completely while much **1** was still present in the matrix as judged by UV and IR spectra. This shows convincingly that the ESR signal is not due to the imine **1**. In the absence of irradiation, the ESR spectrum of the argon matrix remained unchanged for 2 days at 12 K. Similar results were obtained in polyethylene and argon matrices.

The spectral region in which the ESR signal appears is highly characteristic of triplet nitrenes. With the assumption of cylindrical symmetry ($E = 0$), we obtain $|D/hc| = 1.69$ cm^{-1}, a value typical of alkyl nitrenes.[35]

In spite of repeated efforts, we were unable to generate enough of this paramagnetic species to observe its UV or IR spectrum. An experiment in which the matrix was very heavily doped with benzophenone as sensitizer did not produce a stronger ESR spectrum. Clearly, the nitrene is only present in trace amounts.

Additional results compatible with the assignment of the minor photoproduct as adamantylnitrene (**5**) were obtained by chemical trapping. Photochemical changes observed by IR spectroscopy

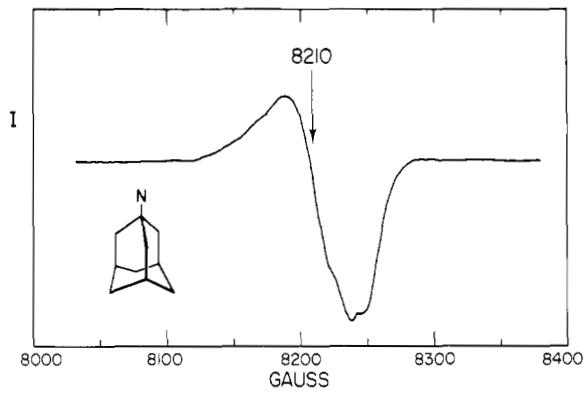

Figure 5. ESR spectrum of **5** in an argon matrix at 12 K (klystron frequency, 9.3 GHz).

on **2** isolated in an argon matrix doped with about 10% of carbon monoxide and irradiated at either 254 or 308 nm were the same as described above for **2** isolated in a matrix of pure argon. After a nearly complete photoconversion of the azide **2** into the imine **1**, and presumably into a trace of the nitrene **5** as well, as suggested by the ESR measurements described above, the matrix was warmed up to 34 K. No changes in the IR spectrum were observed, other than those attributable to annealing processes. At this temperature, matrix-isolated **1** is stable for many hours, while molecules of the size of CO already exhibit considerable translational mobility. When the irradiation was now continued at 34 K, a weak IR band at 2261 cm^{-1} appeared. Its intensity increased for several hours and then remained constant as irradiation was continued, although the amount of **1** present was still essentially unchanged and free CO was still present. This suggests that the peak at 2261 cm^{-1} is not due to a photoreaction of **1**. Also, this peak did not form when the experiment was repeated in the absence of CO in the matrix. The most likely explanation is that it is due to a trace of adamantyl isocyanate formed by photochemical addition of CO to the small amount of nitrene **5** present. Isocyanates are characterized[33b] by an extremely intense band in the region 2242–2274 cm^{-1}, and at low concentrations this should be their only observable IR absorption. Authentic adamantyl isocyanate,[36a] prepared from the amine and phosgene, showed a band at 2261 cm^{-1} in argon matrix. There is precedent for this result in that matrix-isolated pentafluorophenylnitrene has been reported to undergo a photochemical addition of CO to yield pentafluorophenyl isocyanate.[36b]

The stability of the thermally equilibrated triplet nitrene **5** under the conditions of our experiments excludes its involvement as an intermediate in the low-temperature photochemical transformation **2** → **1**. However, singlet nitrene and hot triplet nitrene intermediates cannot be excluded at present.

Matrix Photochemistry of 4-Azahomoadamant-3-ene (1). Very long irradiation of argon or polyethylene matrix-isolated **1** with short-wavelength light ($\lambda < 260$ nm, 2–4 days) results in the gradual loss of its spectral features in UV and IR spectra. At the same time, two new sets of IR peaks appear. The first set, which disappears upon warm-up to 40–50 K, is associated with an ESR signal characteristic of a triplet. The zero-field parameters do not fit a nitrene structure. The second set is stable at least for a brief period of time up to room temperature.

Our original proposal[14] that the latter species is the stable 4-azahomoadamant-4-ene (**6**) was in error: authentic **6** has now been synthesized according to ref 37 and its matrix-isolation spectra were found to differ from those of the more stable component obtained upon irradiation of **1**.

Work on the identification of the two secondary photoproducts formed by extended irradiation of **1** is in progress.

Molecular Structure of 4-Azahomoadamant-3-ene (1). The interesting structural aspect of **1** is the geometry of the C=N

(35) Wasserman, E. *Prog. Phys. Org. Chem.* **1971**, *8*, 319.

(36) (a) Stetter, H.; Wulff, C. *Chem. Ber.* **1962**, *95*, 2302. (b) Dunkin, I. R.; Thomson, P. C. P. *J. Chem. Soc., Chem. Commun.* **1982**, 1192.

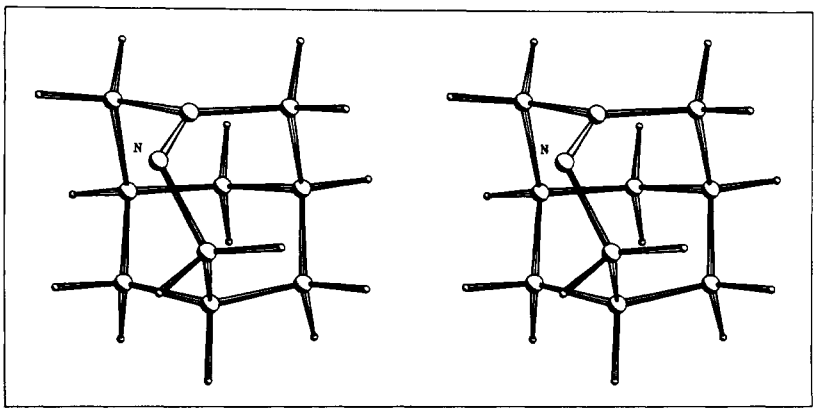

Figure 6. A stereoscopic view of the MNDO-optimized geometry of **1**.

Table I. Results of MNDO Calculations on **1** and **3**[a]

	1	3
pyramidalization angle at C (deg)	8	0
torsion angle (deg)	52	0
C=N–C valence angle (deg)	118	126
C=N bond length (Å)	1.303	1.290
dipole moment (D)	1.08	0.99
charge on C	+0.040	+0.022
charge on N	−0.298	−0.285

[a] At MNDO-optimized geometries.

double bond and its immediate environment. Ordinarily, the $C_2C{=}NC$ moiety prefers to be planar.[20-25,28] If resistance to torsion is at all successful in **1**, the torsion angle will be less than 90° and the equilibrium geometry of **1** will not have a plane of symmetry which one might perhaps expect upon a casual inspection of the usual[5,9] structural representation **1**. Thus, intuition leads us to believe that **1** is a chiral molecule. A geometry optimization by the MNDO method[38] produced the result shown in Table I and Figure 6: the angle of pyramidalization[39] at the "sp^2" carbon is 8°, the torsion angle[40] is 52°, the C=N—C valence angle is 118°, and the C=N bond length is 1.303 Å. These values are compared in Table I with those produced by the MNDO method for the strain-free imine **3**. Clearly, the largest deviation is imposed on the torsion angle, which is calculated to lie half-way to the orthogonality limit. However, the C=N—C valence angle is also noticeably decreased. On the other hand, the C=N bond length is hardly affected. The calculation suggests that the molecule is indeed chiral in its ground electronic state and that the two enantiomers are best represented by the formulas **1A** and **1B**.

While it is not easy to test directly the calculated geometrical structure of a large molecule which has only been characterized in low-temperature matrices, several probes for the correctness of the theoretical result come to mind:

(i) If **1** is chiral, it may be possible to resolve it and measure its circular dichroism.

(ii) IR polarization directions are more or less directly tied to molecular geometry and are experimentally accessible, at least in principle. In particular, the MNDO calculation yields a force field and the dipole moment as a function of geometry[41] and thus predicts vibrational frequencies, including isotopic shifts, IR intensities, and polarizations.

(iii) NMR on a ^{15}N enriched sample of matrix-isolated **1** should yield directly the length of the C=N bond, using principles already tested on other matrix-isolated species.[42]

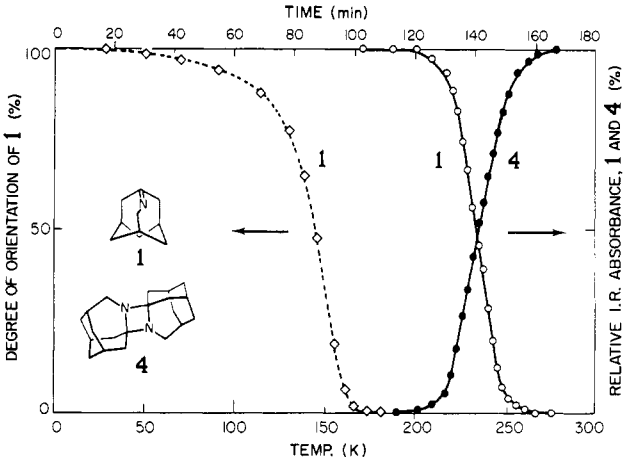

Figure 7. Full lines: time dependence of the relative absorbance due to the IR bands of **1** (decreasing from 100 to 0%) and **4** (increasing from 0 to 100%) contained in a polyethylene matrix after the cryostat has been turned off. Dashed line: time dependence of the polarization degree of the IR bands of **1** initially induced by partial photodecomposition of **2** with linearly polarized 308-nm light, after the cryostat has been turned off. Approximate sample temperature as a function of time is shown at the bottom.

In the present study, we have addressed the first of these issues, (i), and in part also the second issue, (ii). Before launching into a description of the results, we note a pertinent result already obtained in a concurrent investigation of IR transition moment directions in **1**, namely information on the rate of rotational diffusion of **1** in various matrices. When **2** is irradiated with linearly polarized light in an argon matrix or polyethylene sheet at 12 K until about half is converted into **1**, the IR spectra of both **1** and **2** show strong dichroism. At 30 K in an argon matrix, and at about 120 K in polyethylene, it takes about 10 h for the linear dichroism of **1** to disappear. At the same time, the linear dichroism of some but not all IR bands of **2** disappears as well, indicating that its rotation is anisotropic and slower for at least one of its principal rotation axes, as would be expected from its shape. A qualitative feeling for the rate of rotational diffusion of **1** in polyethylene as a function of temperature, adequate for the present purposes, can be obtained from Figure 7 which also gives qualitative information on the rate of dimerization of **1** in polyethylene as a function of temperature. The important conclusion in the present context is that in the temperature range 160–200 K, **1** rotates rapidly in polyethylene on the time scale of seconds or shorter but does not undergo detectable dimerization on the time scale of hours. More quantitative measurements of this type provide information about the temperature dependence of the rate

(37) Sasaki, T.; Eguchi, S.; Toi, N. *Heterocycles* **1977**, *7*, 315.
(38) Dewar, M. J. S.; Thiel, W. *J. Am. Chem. Soc.* **1977**, *99*, 4899, 4907.
(39) Defined here as the angle between any one of the three bonds attached to the bridgehead carbon and the plane perpendicular to the axis of the "π" orbital on this carbon.
(40) Defined here as the dihedral angle between the planes containing the C=N bond and (i) the axis of the bridgehead carbon "π" orbital[38] or (ii) the axis of the nitrogen "π" orbital (perpendicular to the C=N—C plane).
(41) Dewar, M. J. S.; Ford, G. P.; McKee, M. L.; Rzepa, H. S.; Thiel, W.; Yamaguchi, Y. *J. Mol. Struct.* **1978**, *43*, 135.
(42) Zilm, K. W.; Beeler, A. J.; Grant, D. M.; Michl, J.; Chou, T.-C.; Allred, E. L. *J. Am. Chem. Soc.* **1981**, *103*, 2119 and references therein.

of rotational and translational diffusion of solutes in polymers and will be published elsewhere.

Photoresolution. Imines undergo photochemical syn-anti isomerization readily.[20,21] In the case of **1**, such an isomerization is tantamount to the interconversion of the enantiomers: **1A** ⇄ **1B**. A priori, then, one would expect a resolved sample of **1** to be subject to photoracemization with natural or linearly polarized light, which is absorbed equally by **1A** and **1B**. By the same token,[43] a racemic mixture of **1A** and **1B** should be partially photoresolved by irradiation with circularly polarized light, which is absorbed to a different degree by **1A** and **1B**. In the photostationary state reached with left-handed circularly polarized light,

$$\epsilon_L[\mathbf{1A}] = \epsilon_R[\mathbf{1B}] \quad (1)$$

where ϵ_L and ϵ_R are the extinction coefficients of the pure enantiomer **1A** for left-handed and right-handed circularly polarized light at the wavelength used for the irradiation, respectively, and where [**1A**] and [**1B**] stand for the concentrations of the two enantiomers. In the photostationary limit, we have for the resolved fraction

$$[\mathbf{1A}] - [\mathbf{1B}]/([\mathbf{1A}] + [\mathbf{1B}]) = -\Delta\epsilon/2\epsilon \quad (2)$$

where $\Delta\epsilon = \epsilon_L - \epsilon_R$ and $\epsilon = (\epsilon_L + \epsilon_R)/2$, and this corresponds to optical purity of $(50\Delta\epsilon/\epsilon)\%$. The excess enantiomer will be the one which absorbs the left-handed light used for the photoresolution experiment less than right-handed light. The ellipticity θ observed at the wavelength of irradiation will be reduced by the factor $-\Delta\epsilon/2\epsilon$ over that of an optically pure sample

$$\theta = 32.98\Delta\epsilon cl(-\Delta\epsilon/2\epsilon) = -16.49(\Delta\epsilon/\epsilon)^2 A \quad (3)$$

where $A = \epsilon cl$ is the absorbance of the sample at the wavelength of irradiation. Thus, a measurement of A and θ permits the determination of $\Delta\epsilon/\epsilon$.

If right-handed circularly polarized light is used for the photoresolution instead, the ellipticity observed at the wavelength of excitation will be positive but its absolute magnitude reached in the photostationary state will be the same.

Measurements of circular dichroism are severely compromised if the sample also exhibits linear dichroism, even if the latter is very weak.[44] Since we find that irradiation of samples of **1** in matrices at low temperatures where molecular rotation is slow induces strong linear dichroism if linearly or elliptically polarized light is absorbed, it is essential to use as nearly circularly polarized light as possible in the photoresolution experiment on such samples. With some effort, this measurement has been accomplished.[14]

We have since found that it is possible and far easier to work in a polyethylene matrix at temperatures at which the rotational relaxation is rapid and lasting linear dichroism cannot be induced.[45] In the present case of **1**, this implies work above 160 K and below 200 K, where no measurable dimerization occurs on the time scale of the measurement (Figure 7).

When **1** in polyethylene was irradiated at 12 K with circularly polarized 308-nm light from a XeCl excimer laser, no reduction in the intensity of its IR peaks was apparent even after many hours. A clearly detectable CD signal of the anticipated sign, peaking at 301 nm and measured after warmup to about 200 K, appeared after only a few minutes and reached its maximum after about 10 min of irradiation. In addition, another CD peak of the opposite sign was present at 214 nm (Figure 1).

The same CD spectrum was obtained when the irradiation was performed at about 200 K. Upon reversal of the handedness of the light, the signal decreased to zero and then reappeared with opposite sign and reached the same magnitude. The process was repeated several times. The CD spectra were not affected by a rotation of the sample or by rotation of the linear polarizer–Fresnel rhomb assembly which produced the circularly polarized light. Irradiation with unpolarized light at 308 nm caused disappearance of the CD signal as expected. This behavior leaves no doubt that **1** is chiral.

An absolute vertical scale for the CD curve shown in Figure 1 resulted from the observation that the ellipticity at 308 nm measured at the photostationary state was $\theta_{308} = -0.03°$ when the absorbance of the sample at this wavelength was $A_{308} = 1.12$, using eq 3 and $\epsilon = 245$.

Upon raising the temperature, the CD signal disappeared at the same rate as the IR bands of **1** disappeared and those of the dimer **4** appeared. A conservative estimate of the upper limit for the rate of racemization is 10^{-6} s^{-1} at 207 K, and even if the frequency factor were as low as 10^{12} s^{-1}, this implies an Arrhenius activation energy of at least 17 kcal/mol. In simple imines, the barrier for thermal syn-anti isomerization appears to be about 25–30 kcal/mol.[46] It could well be comparable in **1**: the initial state is destabilized by torsion and other strain, but the transition state is also destabilized since the C=N—C valence angle cannot attain its preferred value of 180°. There are no indications that the inability of the C=N—C moiety to reach linear geometry hinders the photochemical syn-anti isomerization, and such hindrance would indeed not be expected if the photochemical isomerization proceeds by torsion.

No experimental information on the relation of the absolute chirality of **1** to the CD sign of the 301-nm band is available. The opposite relative signs of the 301- and 214-nm CD bands (Figure 1) are meaningful, however, and provide a fairly stringent test for the quality of any theoretical description of the electronic states of **1**.

We have also attempted to measure the magnetic circular dichroism of a racemic sample of **1**, using a 1.5-T electromagnet. The observed ellipticity was extremely weak, less than 0.003° for samples of optical density 1.5 at the maximum of the $n\pi^*$ transition, and the effort was abandoned. An upper limit of $2 \times 10^{-5}\beta_e D^2/\text{cm}^{-1}$ can be placed on the absolute value of the B term of the $n\pi^*$ transition. This result, though disappointing, is perhaps not surprising since $n\pi^*$ transitions generally tend to give very weak MCD signals. Attempts to measure in the region of the $\pi\pi^*$ transition were even less successful, due to the weakness of the light source in this spectral range and the much higher extinction coefficient.

Vibrations of 4-Azahomoadamant-3-ene (1). Only a single highly characteristic vibration is expected for structure **1**. This is the C=N stretch already assigned above to the peak near 1600 cm^{-1}, presumably split into a doublet by Fermi resonance (we have found no indication that the splitting might be due to site effects). Preliminary to efforts to determine the polarization directions of this and other IR bands in the molecular framework, which are currently underway and promise to provide some information on the equilibrium geometry, we have compared the measured position and intensity of the IR bands of **1** with those expected from MNDO calculations using the gradient method.[41]

The method was calibrated on the C=N stretch frequency of the unstrained imine **3**. The calculated frequency was about 15% too high and required multiplication by 0.854 in order to coincide with the experimental value, 1669 cm^{-1}. Adopting this multiplicative correction factor for all IR frequencies computed for **1**, we have obtained the theoretical spectrum shown in Figure 1. Although agreement with the observed spectrum is not perfect, the overall spectral line pattern of positions and intensities is reproduced correctly and the theoretical C=N frequency, 1585

(43) Stevenson, K. L.; Verdieck, J. F. *Mol. Photochem.* **1969**, *1*, 271. Norden, B. *Acta Chem. Scand.* **1970**, *23*, 349. Stevenson, K. L. *J. Am. Chem. Soc.* **1972**, *94*, 6652. Kane-Maguire, N. A. P.; Langford, C. H. *Can. J. Chem.* **1972**, *50*, 3381. Porter, G. B.; Sparks, R. H. *J. Photochem.* **1980**, *13*, 123. Zandomeneghi, M.; Cavazza, M., Pietra, F. *J. Am. Chem. Soc.* **1984**, *106*, 7261. For a recent review of asymmetric photochemistry in solution, see: Rau, H. *Chem. Rev.* **1983**, *83*, 535.

(44) Jensen, H. P.; Schellman, J. A.; Troxell, T. *Appl. Spectrosc.* **1978**, 32, 192. Davidson, A.; Norden, B.; Seth, F. *Chem. Phys. Lett.* **1980**, *70*, 313. Kuball, H.-G.; Altschuh, J. *Chem. Phys. Lett.* **1982**, *87*, 599.

(45) Recently, a similar resolution of the experimental difficulties associated with CD measurements in rigid media has been described: Lavalette, D.; Tetreau, C. *J. Phys. Chem.* **1983**, *87*, 3226.

(46) Wurmb-Gerlich, D.; Vogtle, F.; Mannschreck, A.; Staab, H. A. *Liebigs Ann. Chem.* **1967**, *708*, 36. Lang, T. J.; Wolber, G. J.; Bach, R. D. *J. Am. Chem. Soc.* **1981**, *103*, 3275 and references therein.

Table II. Electronic Spectroscopy of **1A**: Experimental and Calculated[a]

	transition			
	"nπ*"		"ππ*"	
property	calcd	exptl	calcd	exptl
transition energy (cm^{-1})	26300	33100	44200	46700
oscillator strength	0.033	0.01	0.189	~0.1
polarization (deg)	71[b]		6[c]	
rotatory strength (β_eD)	0.45	0.43	−0.38	<0
B term[d] 1 ($\beta_e D^2/cm^{-1}$)	-2.5×10^{-5}	~0	7.3×10^{-5}	~0
B term[f] 2 ($\beta_e D^2/cm^{-1}$)	-1.3×10^{-5}		-4.1×10^{-5}	

[a] INDO/S at MNDO-optimized geometry. [b] Angle from C=N–C plane. [c] Angle from C=N bond. [d] Origin of coordinates at the center of gravity. [e] $|B| < 2 \times 10^{-5}$. [f] Origin of coordinates at the N atom.

cm^{-1}, lies surprisingly close to the observed value, ~1600 cm^{-1}. Also the theoretical isotopic shift, 22 cm^{-1}, agrees nicely with the observed value, 18 cm^{-1}. The calculated normal mode motion involves almost exclusively the stretching of the C=N bond, both in **1** and in **3**.

The significance of the agreement between the scaled theoretical result and the experimental spectrum should not be overestimated. Still, the agreement lends credence to the MNDO treatment and to the MNDO equilibrium geometry. Thus, we are inclined to believe that the torsion in **1** indeed lies about halfway between planarity and orthogonality and that the C=N—C valence angle is somewhat reduced from its usual value.

Electronic Structure of 4-Azahomoadamant-3-ene (1). Some of the results on ground-state electron distribution obtained from the MNDO calculations are collected in Table I. The corresponding experimental data are presently lacking; it is hoped that an at least partial test will be provided by the measurement of IR transition moments.

The currently available evidence for the electronic structure of **1** consists of the UV and CD spectra and thus involves both the ground and excited electronic states. In order to interpret these spectra, we have performed calculations by the INDO/S method,[47] assuming the equilibrium ground-state geometry optimized by the MNDO method.[38] The results are summarized in Table II and shown in Figure 1 for comparison with the experimental spectra.

The agreement for excitation energies and relative intensities is fair. The computed weak transition at 26 300 cm^{-1}, polarized approximately perpendicular to the C–N–C plane, can be called "nπ*". It is assigned to the weak observed transition centered at 33 200 cm^{-1} ($f = 0.01$). The computed vertical transition energy is too low by ~7000 cm^{-1}. This may be due to inaccuracies in the assumed geometry obtained from the MNDO minimization or to inadequacies of the INDO/S method, or both. The use of the same procedure (MNDO optimized geometry, INDO/S spectral calculation) on **3** yields an nπ* excitation energy of 30 000 cm^{-1}, to be compared with the value ~42 000 cm^{-1} considered standard[20] for imines with three alkyl substituents, a similar and even larger discrepancy. The procedure thus reproduces the direction of the spectral shift due to bond twisting, but it clearly still leaves much to be desired in terms of quantitative agreement. For molecules of this size, it is difficult to do better with current theoretical tools.

The computed six times stronger transition located at 44 200 cm^{-1} and polarized approximately along the C=N bond can be called "ππ*". It is assigned to the strong observed transition at 46 700 cm^{-1} ($f = 0.1$). A similar calculation for **3** yields a ππ* excitation energy of 56 400 cm^{-1}, to be compared with the value 55 000 cm^{-1} normally quoted[20] for the ππ* transition in imines with three alkyl substituents. In our experience, the INDO/S method generally does better for the energies of ππ* excitations than for those of nπ* excitations, which are often predicted too low. Still, qualitative trends are usually predicted correctly for both.

(47) Ridley, J.; Zerner, M. *Theor. Chim. Acta* **1973**, *32*, 111. Calculation of optical activity followed the procedures outlined by West et al.: West, R.; Downing, J. W.; Inagaki, S.; Michl, J. *J. Am. Chem. Soc.* **1981**, *103*, 5073.

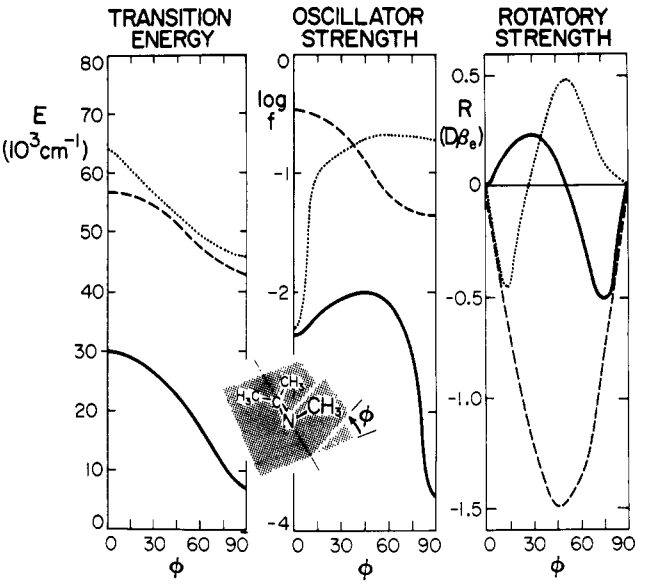

Figure 8. INDO/S-calculated singlet–singlet electronic transition properties of **3** as a function of twist angle φ (degrees): full line, first transition; dashed line, second transition; and dotted line, third transition.

The calculated MCD intensity of both transitions is extremely small and clearly unreliable with respect to sign, which depends on the choice of origin of coordinates within the molecule (for stronger MCD effects this origin dependence still exists but its effect is generally negligible as long as the origin is kept within the molecule[48]). This result is compatible with our observation that the MCD spectrum of **1** is too weak to measure on our instrument ($|B| < 2 \times 10^{-5} \beta_e D^2/cm^{-1}$ for the nπ* transition).

The agreement of the computed and observed CD signs in Figure 1 is encouraging since optical activity usually is relatively difficult to calculate. Being an inherently dissymmetric chromophore, and exhibiting a very large rotatory strength for both transitions, **1** is likely to represent an exceptionally favorable case for a simple theoretical treatment. Certainly, the fact that the signs of the nπ* and ππ* transitions are opposite is clearly reproduced by the theory. The perfect agreement in the calculated magnitudes is undoubtedly fortuitous, but it is pleasant to note all the same. The calculations suggest strongly that the enantiomer **1A** is the one with a positive nπ* and negative ππ* CD band, but we have no way of checking this experimentally.

The Effect of Torsion on the Electronic Structure of the C=N Bond. While the reasonable agreement between the calculated and observed UV and CD spectra of **1** is encouraging, it does not in itself bring much insight into the nature of the electronic states involved. We have sought qualitative understanding of the effects of torsion by analyzing a series of model calculations on **3** at its equilibrium planar geometry, as optimized by the MNDO method, and a series of geometries in which the C=N double bond was gradually rotated out of plane to orthogonality. During the rotation, the initially slightly different lengths of the syn and anti C–C bonds were stepwise brought to equality, which was reached at 90°, and all other bonds and angles were left intact. This appeared sensible in this first attempt, although eventually also the effects of changes in the C=N—C valence angle and in the degree of pyramidalization on the unsaturated carbon need to be investigated. A comparison with ab initio calculations of excitation energies of formaldimine (CH_2=NH)[25,28] performed for a similarly constrained series of geometries provided a check that the INDO/S results are qualitatively reasonable, assuming that the three methyl groups in **3** cause only minor changes relative to the parent formaldimine, such as an overall decrease in excitation energies. The excitation energies *E*, oscillator strengths *f*, and rotatory strengths *R* of **3** calculated as a function of the torsion angle φ are shown in Figure 8. Only the range φ = 0° to 90° is shown since the structures with angles φ and 90 - φ are enantiomers of each other. We do not show the calculated results

for MCD B terms which are very small, are significantly affected by the choice of the origin of the coordinate system, and behave erratically as a function of ϕ.

State Energies. The interpretation of the INDO/S results for the lowest energy singlet–singlet transition is straightforward. The decrease of the excitation energy with increasing torsion angle ϕ is due both to an increase in the energy of the ground state, which has a rotational barrier, and to a decrease in the energy of the excited state, which has a minimum at the position of orthogonal twist, $\phi = 90°$, at least when viewed along the one-dimensional cut through the multidimensional nuclear configuration space considered here. A multidimensional search for the location of the equilibrium geometry of the excited singlet state is still underway, but it is already possible to say that the twisting motion is indeed plausible as a mechanism for the photochemical syn-anti isomerization and that the equilibrium geometries are very different in the ground electronic state and in the $n\pi^*$ state.

The change of the excitation energy with the torsion angle ϕ calculated here for **3** is qualitatively similar to that calculated in ref 28 by a much more reliable method for the parent imine, $CH_2{=}NH$. Both calculations suggest that the 9000-cm^{-1} shift of the $n\pi^*$ transition to lower energies caused by going from ordinary planar imines with three alkyl substituents (excitation energy about 42 500 cm^{-1})[20-23] to **1** (excitation energy about 33 200 cm^{-1}) corresponds to going about half-way from planarity to orthogonality, thus approximately to $\phi = 45°$. This agrees with the twist angle of 52° obtained from the MNDO geometry optimization described above. This argument in favor of the half-way twisted geometry in **1** is only qualitative since it ignores the effects of possible differences in other geometrical parameters such as the C=N—C valence angle. That these differences should play some role is indicated by a comparison of the excitation energy calculated for **3** at 52° twist ($\sim$22 000 cm^{-1}) and that calculated for **1** at its equilibrium geometry which involves not only a 52° twist but other distortions as well (26 300 cm^{-1}).

The interpretation of the INDO/S results for higher energy singlet–singlet transitions is complicated by the fact that for torsion angles ϕ larger than about 30°, a superposition of two nearly degenerate transitions seems to correspond to the observed $\pi\pi^*$ band. Thus, what clearly is a $\pi\pi^*$ transition at planar imine geometry acquires a mixed $\pi\pi^*$–$\sigma\pi^*$ character at larger twist angles. This was not found in the ab initio calculations[28] on $CH_2{=}NH$, perhaps as a result of the absence of the three methyl groups. It is also quite possible that the INDO/S result for the $\sigma\pi^*$ configuration is spurious. In the following, we assume that either the contributions from the two nearly degenerate calculated transitions add up in the observed spectra or else only the $\pi\pi^*$ transitions is actually present.

Either way, a decrease in the excitation energy of the second band with increasing torsion angle ϕ is expected from our calculation and also from the ab initio calculation on $CH_2{=}NH$.[28] Both calculations are compatible with the notion that the large shift of the $\pi\pi^*$ transition energy to smaller values in **1** (46 700 cm^{-1}) relative to the only poorly documented value of 55 000 cm^{-1} usually quoted for planar imines with three alkyl substituents[20-23] is due to a large increase in the torsion angle ϕ. The magnitude of the shift derived from the two above numbers is again about 9000 cm^{-1}, similar to the $n\pi^*$ shift, but it is now much less certain due to the questions that exist concerning the assignment of the $\pi\pi^*$ band in planar imines. Comparison with the results of either calculation, INDO/S for **3** or ab initio for $CH_2{=}NH$, suggests a torsion angle ϕ in the vicinity of 60° if the effect of other geometrical changes is again ignored.

Taking the evidence from the MNDO geometry optimization along with the evidence from the shifts of the $n\pi^*$ and $\pi\pi^*$ transitions, we propose that a reasonable interim value for the torsion angle in **1** is 50 ± 10°. Further work will be necessary before this can be refined to satisfactory accuracy.

Oscillator and Rotatory Strengths. The other calculated spectral properties of **3** (Figure 8) change in even more interesting ways as a function of the torsion angle ϕ. The intensity of the $n\pi^*$ transition should first increase by about a factor of 2, reach a maximum near $\phi = 45°$, and then decrease until at $\phi = 90°$ it should be an order of magnitude less than initially, at $\phi = 0°$. The extinction coefficient we find for **1** ($\epsilon = 245$) is only marginally higher than that usually quoted[20] for planar imines with three alkyl substituents ($\epsilon \cong 200$). The prediction of the intensity of the second transition is somewhat confused by the presence of two transitions of nearly the same calculated energy, but there is no doubt that it should decrease slowly as ϕ increases. The observed decrease of the extinction coefficient to about $\epsilon \cong 3 \times 10^3$ in **1** relative to the value usually quoted[20] for planar imines with three alkyl substituents, $\epsilon \cong 10^4$, is in the expected direction.

For all values of ϕ, the calculated polarization directions remain roughly perpendicular to the C=N—C plane for the $n\pi^*$ transition and roughly parallel to the C=N bond direction for the $\pi\pi^*$ transition. We presently have no experimental results bearing on this.

The calculated rotatory strengths of the $n\pi^*$ and $\pi\pi^*$ transitions behave in a particularly interesting way as a function of ϕ. They clearly must vanish for $\phi = 0°$ and 90° since in these two situations **3** has a plane of symmetry. The $\pi\pi^*$ transition keeps the sign of its rotatory strength in this quadrant and switches to the opposite sign as ϕ goes into the next quadrant, $\phi = 90°$ to 180°. This is true whether we take it to be represented by a sum of both nearly degenerate transitions calculated in this region or whether we only take the stronger contribution. In a sense, then, the $\pi\pi^*$ transition follows the same kind of a "quadrant rule" as, for instance, the first $n\sigma^*$ transition of the disulfide chromophore.[49] The calculated behavior of the rotatory strength of the $n\pi^*$ transition is more intriguing in that it starts at zero at $\phi = 0°$, acquires one sign as ϕ grows, reaches an extremum value near $\phi = 30°$, decreases to zero near $\phi = 50$–55°, acquires the opposite sign as ϕ grows further, reaches a new extremum near $\phi = 75°$, and then drops precipitously to zero as ϕ approaches 90°. To our knowledge, this peculiar behavior is unprecedented. Before a detailed discussion of its origin in terms of the molecular orbitals of a twisted imine can be justified, we feel that it is necessary to explore the effects of other geometrical variables, such as the C=N—C valence angle, which are likely to affect the value of the twist angle at which the sign switch occurs. Also, we need to find experimental evidence that the peculiar trend predicted by the approximate theory is indeed real. The experimental investigation is facilitated by the availability of the $\pi\pi^*$ transition as an internal standard. Thus, we expect that for small torsion angles ϕ the CD signs of the $n\pi^*$ and the $\pi\pi^*$ transitions will be mutually opposite while for large torsion angles they will be the same. In this regard, **1** represents the first piece of experimental evidence and is a representative of the "small torsion angle" category.

Molecular Orbitals of a Twisted Imine. Although we have postponed a detailed analysis of the origin of the torsion angle dependence of the various observables displayed in Figure 8, it appears worthwhile to emphasize an important difference between the simple MO or VB description of the twisting of a C=C bond and of a C=N bond, which is not always appreciated in the published literature. In their respective ground states, the former becomes a single σ bond at orthogonality while the latter remains a double bond, albeit one with a significantly weakened π component. In this sense, the twisting of the C=N bond is analogous to the pyramidalization of one of the termini of a C=C bond and not to its twisting.

The C=C bond can be most simply modeled as a two-orbital two-electron π system plus a collection of immutable σ bonds (Figure 9). It possesses a bonding π MO and an antibonding π^* MO which are degenerate at the torsion angle $\phi = 90°$. Both the MO and the VB description produce three singlet states and a triplet state in this model, and these are sufficient for the qualitative understanding of much of the behavior of simple olefins, both in the ground and in the excited states.

On the other hand, even the simplest model useful for the description of the twisting of a C=N bond already requires the

(48) Warnick, S. M.; Michl, J. *J. Am. Chem. Soc.* **1974**, *96*, 6280.
(49) Linderberg, J.; Michl, J. *J. Am. Chem. Soc.* **1970**, *92*, 2619.

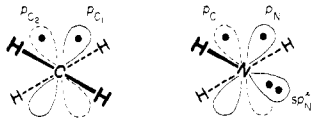

Figure 9. Newman projection of the basis set orbitals used to model the C=C and the C=N bonds. Approximate occupancies in the ground state are shown.

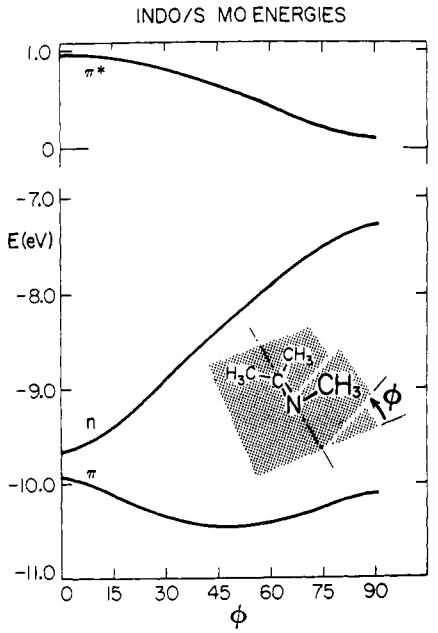

Figure 10. INDO/S MO energies of the frontier orbitals of **3** as a function of the twist angle ϕ (degrees).

use of four electrons in three interacting orbitals, plus a collection of inert σ bonds (Figure 9). The "lone pair", or "n", AO on nitrogen (more accurately, an sp^x_N hybrid orbital) has a zero resonance integral with the "π" AO on nitrogen (more accurately, a p_N orbital) and does not interact with it. However, at general values of ϕ, both of these nitrogen orbitals interact with the "π" orbital on the unsaturated carbon (an sp^y_C hybrid orbital if the carbon is pyramidalized). The labels "π" and "n" are appropriate only at $\phi = 0°$, and we shall now replace them with the more descriptive labels sp^x_N, p_N, and sp^y_C. To a good approximation, the hybridization exponent x is determined by the C=N—C valence angle. For 120°, $x = 2$, and for 180°, $x = \infty$, implying a pure 2p orbital. For 90°, $x = 0$, implying a pure 2s orbital. Similarly, the exponent y is determined by the degree of pyramidalization at the carbon atom. For no pyramidalization, $y = \infty$, implying a pure 2p orbital. For tetrahedral pyramidalization, $y = 3$.

In the absence of pyramidalization on carbon, the sp^x_N–sp^y_C interaction vanishes at $\phi = 0°$ while the p_N–sp^y_C interaction is maximized. The resulting MO's of the planar system are π and π^* from the latter interaction, and sp^x_N as the lone pair orbital (Figure 10). Low-energy singlet configurations are $\pi^2(sp^x_N)^2$ which dominates the ground state, $\pi^2(sp^x_N)^1\pi^{*1}$ which dominates the $n\pi^*$ state, and $(sp^x_N)^2\pi^{*1}$ which dominates the $\pi\pi^*$ state.

For any degree of pyramidalization on carbon, the sp^x_N–sp^y_C interaction is maximized at $\phi = 90°$ while the p_N–sp^y_C interaction vanishes. The resulting MO's of the orthogonal system are π and π^* from the former interaction and p_N as the lone-pair orbital. Low-energy singlet configurations are $\pi^2p_N^2$ which dominates the ground state, $\pi^2p_N^1\pi^{*1}$ which dominates the $n\pi^*$ state, and $\pi^1p^2_N\pi^{*1}$ which dominates the $\pi\pi^*$ state (Figure 10). Thus, a π bond is still present in the ground state. In general, it will be weaker at orthogonality than it was at $\phi = 0°$, since the sp^x_N–sp^y_C overlap may be quite poor, depending on the C=N—C valence angle. At a particular value of this angle, the ground and $n\pi^*$ states are expected to be degenerate, providing a "funnel" for efficient return of an excited imine to the ground state in a photochemical process. An important factor contributing to a high total energy at $\phi = 90°$ in the ground state is the lone pair which is housed in a higher energy orbital (pure 2p instead of a hybrid in the present crude model; in a better description of the ground state the 2p orbital on nitrogen interacts with other MO's of σ symmetry[50]). Note that this factor contributes to the rotational barrier in the ground state but will not tend to make the C=N bond longer. This suggests a rationalization for the very small increase in the C=N bond length calculated for **1** relative to **3** (0.01 Å).

At intermediate values of the torsion angle, $0° < \phi < 90°$, all three basis set orbitals, p_N, sp^x_N, and sp^y_C, mix and yield three MO's (Figure 10). In the Hückel model, the system is topologically equivalent to the allyl anion but the electronegativities of the three centers differ. That of p_N is given by the properties of the 2p AO on nitrogen, that of sp^x_N is a function of the C=N—C valence angle, and that of sp^y_C is a function of pyramidalization on the carbon atom. The gradual twisting from $\phi = 0°$ to 90° is analogous to a coupled twisting of bonds in the allyl anion, starting with the C_1—C_2 bond orthogonal, proceeding through both the C_1–C_2 and C_2–C_3 bonds partially twisted, and ending with the C_2–C_3 bond orthogonal.

Conclusions

The results of this study represent the first detailed spectroscopic characterization of a highly twisted C=N bond. Both the vibrational spectra (Raman, IR) and the electronic spectra (UV absorption, CD) of 4-azahomoadamant-3-ene (**1**) show large shifts relative to unstrained simple imines and agree with theoretical expectations based on a combination of the MNDO and INDO/S methods. This lends support to the MNDO result for the equilibrium geometry of **1**, which features a 52° twist angle around the C=N bond.

Experimental Section

Melting points were taken on a Hoover apparatus and are uncorrected. ^{1}H NMR spectra were obtained on a Varian EM 360 L instrument and room-temperature IR spectra on a Nicolet MX-1 instrument.

Materials. Adamantyl Azide and Adamantyl Azide-^{15}N. 1-Azidoadamantane was prepared according to the method of Sasaki et al.[51] with some modifications. An ice-cooled solution of 1-adamantanol (15.2 g, 0.1 mol) (99%, Aldrich) in 100 mL of chloroform was stirred with 100 mL of 65% aqueous H_2SO_4, with an efficient mechanical stirrer (400–700 rpm). To this mixture 13.0 g (0.2 mol) of solid sodium azide (99%, Aldrich) was added in small portions. The mixture was vigorously stirred at room temperature for 7 h and monitored by GLC. The chloroform layer was separated, and the aqueous layer was extracted twice with chloroform. The combined chloroform layer was washed with water, 5% $NaHCO_3$, and again with water and then dried. Removal of solvent by rotatory evaporation left a crude yellowish product which sublimed (100 °C (0.3 torr)) to yield 88–93% of white 1-azidoadamantane, mp 79–80 °C. The analytical sample, recrystallized from cyclohexane, melted sharply at 81 °C.

The labeled azide was prepared essentially in the same manner (using 0.38 g, 2.5 mmol) of 1-adamantanol: 0.3 g, 4.6 mol of $Na^{15}NN_2$ sodium azide (Norell Inc.), 4 mL of chloroform, and 10 mL of 65% H_2SO_4.

4-Azahomoadamant-4-ene. To a mechanically stirred and ice-coled mixture of 98% methanesulfonic acid (33 mL) (Aldrich) and chloroform (22 mL) were added 1.14 g (17.5 mmol) of sodium azide and 2.0 g (13.14 mmol) of 2-adamantanol, obtained from adamantanone and $NaBH_4$ in methanol. Then sodium azide (2.28 g, 35.1 mmol) was introduced portionwise during 0.5 h. After stirring was continued for 10 h at room temperature, the mixture was poured onto ice water. The chloroform layer was separated, and the aqueous layer was extracted twice with chloroform. Evaporation of the dried organic layer yielded no organic material. The aqueous layer was treated with concentrated KOH and ice producing a precipitate which was filtered, dried, and purified by two sublimations. The yield of the crude product which melted at 225–230 °C was 1.52 g (77%). The sublimed product melted at 255–257 °C with decomposition and partial sublimation (lit. mp 215–218 °C,[37] 231–234 °C[52]). The NMR and IR spectra were essentially identical with those of the authentic material.

(50) Bach, R. D.; Wolber, G. J. *J. Org. Chem.* **1982**, *47*, 239, 245 and references therein.
(51) Sasaki, T.; Eguchi, S.; Katada, T.; Hiroaki, O. *J. Org. Chem.* **1977**, *42*, 3741.
(52) T. Sasaki, personal communication.

An initial attempt in which a smaller amount of sodium azide was used (25 mmol of 2-adamantanol and 31 mmol of NaN_3) gave 52% of 2-adamantyl methanesulfonate isolated from the chloroform layer. The ester was purified by sublimation: mp 58–60 °C (lit. mp 63–65 °C,[53] 46–48 °C[54]); ^1H NMR ($CDCl_3$) δ 1.3–2.2 (m), maximum at 1.75 (14 H), 2.95 s (3 H), 4.8 s (1 H); IR (KBr) 2933, 2912, 1342, 1187, 1173, 987, 962, 923, 905, 873, 547, 531 cm^{-1}. The spectral data were essentially identical with those reported.[53]

Polyethylene. Pellets of linear low-density polyethylene were obtained from Dow Chemical Co. and were hot-pressed at 150–160 °C into sheets of 0.3–0.8-mm thickness for most IR absorption measurements.[55] They were annealed at 85 °C in the hot press overnight.

Argon and nitrogen gases were purchased from Matheson, and their purity was 99.9995%.

3-Methylpentane (Phillips Petroleum Co.) was refluxed with sodium, distilled, and passed over an Al_2O_3–$AgNO_3$ column. Solutions were degassed by five freeze–pump–thaw cycles on a vacuum line.

Matrix-Isolation Photochemistry and Spectroscopy. Argon and nitrogen matrices were prepared on windows, plates, or rods attached to the cold tip of an Air Products CS-202 Displex closed-cycle helium cryostat with indium gaskets. Standard vapor mixing and deposition techniques were used. Deposition rates were about 0.5 mmol/min. Argon deposition temperatures were 24 K for a sapphire window (UV), 29 K for a CsI window (UV, IR, Raman) and for an Ag plate with a narrow CsI window, used for simultaneous IR and Raman work, and 18 K for a Cu rod, used for ESR measurements. Nitrogen deposition temperature was 26 K for a CsI window. Irradiation and spectral measurements were performed at 12–13 K.

Temperatures were measured by using a 0.07% iron-doped gold–chromel thermocouple located at the tip of the cold end of the cryostat. Accuracy was better than ± 2 K. The thermocouple was calibrated against an ice–water mixture and against the temperature of liquid nitrogen, corrected for measured atmospheric pressure. The actual sample temperature was higher than that measured. The difference was a function of the window holder and window material used. In the case of the worst heat conductor, polyethylene, the difference was measured directly by inserting a second thermocouple into the sheet and was found to be less than 2 K at 12–13 K. During the "free" warm-up (Figure 7) the difference never exceeded 4 K.

Polyethylene sheets were first kept in the vapor of **2** at room temperature for a suitable length of time (typically 30 min for UV and up to 10 h for IR work). A sheet was then mounted on the cryostat tip, (i) between two copper plates with a 5 × 12 mm opening in the center and no windows (for CD and UV measurements), or (ii) between two thin (1.2 mm) CsI plates (for IR measurements), or (iii) between a standard nickel-plated copper Raman sample holder and a copper sheet with an opening in the center. The cryostat was purged with argon for 30–60 min, the tip cooled to 200 K, the argon pumped out, and the tip with the mounted sample cooled to the desired working temperature. Such samples were essentially air-free (no CO_2 band detectable by IR). This procedure minimized evaporation losses which are otherwise significant even if the sheet is kept mounted between two optical plates. When desirable for keeping product spectral intensities within optimum range, the optical density of the starting material in the sheet was first reduced by keeping the sheet at room temperature under reduced pressure of argon for a suitable length of time.

Except for minor spectral shifts attributed to solvent effects, the IR, Raman, UV, and ESR spectra were the same in argon, nitrogen, and polyethylene matrices. A deliberate addition of 1% of dry air into the argon had no effect on any of the spectra, except that a strong CO_2 peak appeared in IR and O_2 and N_2 peaks appeared in Raman.

3-Methylpentane glass was prepared in degassed Suprasil quartz cells immersed in a quartz dewar equipped with Suprasil windows and filled with liquid nitrogen. This medium was used only for UV measurements.

The photochemical light sources used were a low-pressure mercury lamp for 254 nm, a Lambda-Physik EMG-102 excimer laser for 308 and 249 nm, and a full spectrum of a high-pressure 2.5 kW Hg–Xe lamp for the photodestruction of matrix-isolated **1**. Glan-Thompson prisms and a Fresnel rhomb were used to manipulate the state of polarization of the laser light.

The UV–visible spectra were recorded on a Cary 17 spectrophotometer interfaced to a PDP-11/23 computer, the CD and MCD measurements were made on a Jasco J-500C spectropolarimeter equipped with a 15-kG electromagnet and a microprocessor and interfaced to the PDP computer, the IR spectra were recorded on a Nicolet 6000 series Fourier-transform spectrometer, the Raman spectra were excited with a Spectra Physics argon ion laser (488 nm, 1.5 W) and recorded on a Spex Ramalog 4 spectrometer interfaced to the Nicolet computer in the FT-IR spectrometer, and the ESR spectra were recorded on a Varian V-4502 spectrometer.

All spectra were taken numerous times at a variety of concentrations of the starting azide and at a variety of degrees of conversion in order to bring out all spectral detail, including strong and weak bands. The spectra shown in the figures are the optimum choices for each of the spectral methods and were not all obtained on the same sample. However, at least some of the characteristic peaks in the UV, IR, and Raman spectra were indeed all observed on the same sample in three matrix materials, nitrogen, argon, and polyethylene. For instance, at the high concentration optimal for Raman measurements, the $n\pi^*$ band could be recorded in the UV but the $\pi\pi^*$ band was out of scale, and many IR bands could be recorded but the most intense ones were out of scale. The more dilute sample used to obtain the full UV spectrum ($n\pi^*$ and $\pi\pi^*$) was still suitable for IR measurements but not for Raman, etc. The highest doping levels used were about 1%.

MO calculations were performed on a College of Science DEC 20/60 computer with programs developed by us and programs adapted from those kindly supplied by Professors Zerner (University of Florida) and Dewar (University of Texas).

Acknowledgment. We are grateful to Professor T. Sasaki (Nagoya) for providing the IR and NMR spectra of 4-azahomoadamant-4-ene and to Professor Quast (Würzburg) for a sample of the dimer of 4-azahomoadamant-3-ene. The work at Utah was supported by the National science Foundation (CHE 81-21122) and by the National Institutes of Health (GM 29984). Acknowledgment is made to the donors of the Petroleum Research Fund, administered by the American Chemical Society, for support of the work at Wisconsin.

Registry No. 1, 85557-08-0; **2**, 24886-73-5; **2**-^{15}N, 93685-04-2; **4**, 55086-04-9; **5**, 93685-05-3; **6**, 65218-91-9; 1-adamantanol, 768-95-6; 2-adamantanol, 700-57-2; 2-adamantyl methanesulfonate, 31616-68-9.

(53) Babler, J. H.; Moormann, A. E. *J. Org. Chem.* **1976**, *41*, 1477.
(54) Crossland, R. K.; Servis, K. L. *J. Org. Chem.* **1970**, *35*, 3195.
(55) Radziszewski, J. G.; Michl, J. *J. Phys. Chem.* **1981**, *85*, 2934.